Evaluation of Mechanical Properties of Additive-Manufactured Stainless Steel for Nuclear Applications

Jung-Min Kim[a], Junhyun Kwon[a]*, Hyung-Ha Jin[a]
[a]*Korea Atomic Energy Research Institute, 989-111 Daedeok-daero, Daejeon, 34057, KOREA*
**Corresponding author: jhkwon@kaeri.re.kr*

1. Introduction

Additive manufacturing (AM) is defined as a process of joining materials to make objects from 3D model data, layer by layer, as opposed to conventional subtractive manufacturing methodologies [1]. Most AM technologies usually apply powder or wire as a feedstock which is selectively melted by a focused laser or electron beam and consolidated in following cooling to form an object. With the advantages of rapid forming near-net shape parts without pre-treatment, the AM has recently provided a promising way of potential fabrication of complicated parts. AM has received great interest in aerospace, automotive, medical and nuclear industries. The nuclear industry recognizes its potentials to produce reactor components with enhanced performance and reduced supply chain. The AM transforms rapidly from prototyping to manufacturing applications, which require not only information of the process itself, but also the properties of AM parts depending on the process parameters. However, limited results are available about the AM materials, which are required for the industrial applications.

The core components in a nuclear reactor are essential for a safe operation, which have several interfaces. All interfaces need to be inspected in detail to ensure a safe operation. The rod cluster control assembly (RCCA) must be compatible with the control rod drive mechanism (CRDM), as well as the control rod guide assembly (CRGA). During the reactor operation, the RCCA is moved up and down by means of the CRDM to control the nuclear chain reactions [2]. The CRGA is located in the upper core and is composed of several connected plates with holes that have a fitted form of the RCCA spider, which are called the guide cards [3]. Therefore, their geometrical compatibility should be checked regularly. In US pressurized water reactors (PWR), the RCCA and guide cards were found to be damaged by impact-sliding wear due to flow-induced vibration which generate metal-to-metal contacts [4]. The wear phenomena that occurred to guide cards by the control rod cladding become an emerging issue in the PWR industry.

Austenitic 304L stainless steel (SS) is used extensively inside the reactor pressure vessel. The target component, the PWR guide card, is made of SS 304L. This alloy has long been used in the nuclear industry because of its high corrosion resistance and strength. The objective of our goal is to manufacture a new guide card with 3D printing that is designed to reduce flow-induced vibration. Prior to making objects, however, it is required to evaluate the basic properties of 3D-printed materials. While extensive work has been conducted regarding AM of SS 316L [5-7], little work has been done for the evaluation of SS 304L. In addition, we employ two metal AM methods, including Powder Bed Fusion (PBF) and Directed Energy Deposition (DED), for a benchmark study. In this study, we performed the various mechanical tests of stainless streels made by PBF and DED methods, as well as the microstructural analysis. In addition, pin-on-disk wear test were conducted to examine the wear resistance of those samples.

2. Additive manufacturing methods

The PBF and DED processes have their advantages and disadvantages. Depending on the features of a target object, we have to choose the proper method. The characteristics of each process are described briefly in this section.

2-1. Powder Bed Fusion (PBF)

PBF is an additive manufacturing process in which thermal energy selectively fuses regions of a powder bed [1]. The PBF selectively dissolves the section of the 3D model by applying a thin powder to the bed and scanning a heat source such as a laser or electron beam [8]. When one section is completed, the fabrication positon is lowered down by the thickness of the powder layer. The process of applying powder and irradiating the heat source (laser or electron beam) is repeated to make parts until the entire 3D form is completed. The schematic system and melting process of the PBF is shown in Fig.1. The PBF has a strength in creating complex structures and good surface finish and can make slightly overhang structure due to powder acts as support material. Besides, the disadvantage to the PBF is the slow stacking speed.

2-2. Directed Energy Deposition (DED)

In the DED process, focused thermal energy is used to fuse materials by melting as they are being deposited [1]. DED is a process that metal powder or wire combines with an energy source, typically laser to deposit material directly onto a build tray or an existing part. Because DED resembles welding, it is mainly used for metal and alloy [10]. The process of DED as the

nozzle moving along the path is shown in Fig.2. Due to the nozzle of DED machine attached on a multi axis arm, DED can move freely in multiple directions, which makes DED applicable to large parts and effective for repairing and adding features. The disadvantages of the DED are that the surface condition of the manufactured parts is coarse and the resolution is low. Also the DED process cannot make overhang structure without supports [10].

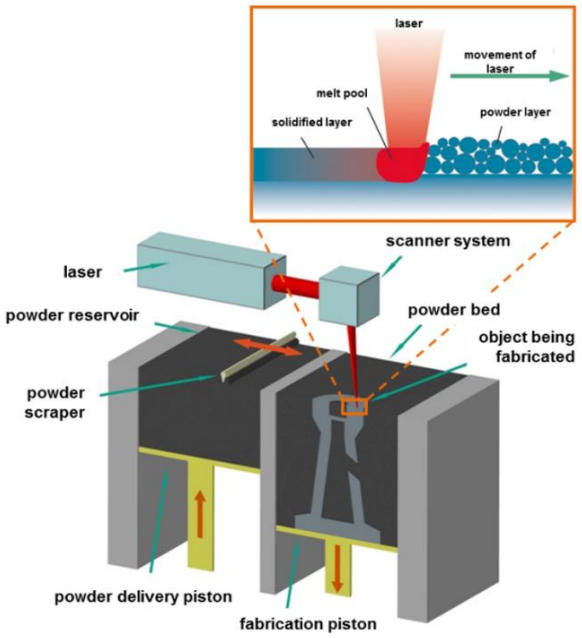

Fig. 1. PBF process and system scheme [9].

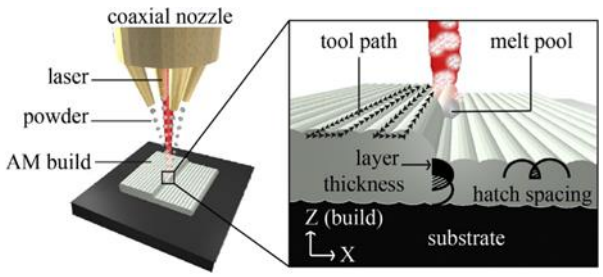

Fig. 2. Schematics of the DED process [11].

3. Experimental

SS 304L metallic powder was prepared depending on the AM methods of PBF and DED. In the PBF process, we used spherical SS powder with an average particle size (15~ 45 μm) supplied by ChangSung Corporation. The specimens were made using a PBF machine M2 (Concept Laser, US). The process conditions are as follows; layer thickness of 30 μm, laser a power of 180 W and scan speed 800 mm/s. In the DED process, we used the SS 304L powder provided by CARPENTER, which has a distribution of particle size between 45 and 150 μm. The specimens were manufactured using a DED machine MX-400 (InssTek, Korea). The process conditions are: feed rates of 2.5 to 3.0 g/min, laser power of 450 W and scan speed 14.2 mm/s.

SS 304L PBF and DED specimens were prepared for microstructural observation by wet grounding with SiC papers followed by vibratory-polishing. Microstructure was assessed by an optical microscope connected to a computer for the pore analysis. And Electron backscattered diffraction (EBSD) patterns were obtained using an EBSD detector from EDAX mounted on a JSM-7200F scanning electron microscope (SEM) operating at an accelerating voltage of 20 kV.

Microhardness measurements were performed using HM-122 Micro Hardness Tester (AKASHI, Japan) with a load of 1 kgf during 10 seconds. The measured hardness values are average of 40 indentations per sample. Then the tensile tests were performed at room temperature with strain rate of 0.005/s. The tensile specimens were extracted from the samples in a direction perpendicular to the building direction. The wear tests on AM SS 304L carried out based on the ASTM standard G99 [12], which is about method for wear testing with a pin-on-disk. The applied normal load was 30 N, and sliding velocity was kept at about 0.22 m/s. The tests were run for a sliding distance of 1.6 km at two different temperatures (25ºC, 250ºC).

4. Results

4-1. Microstructural Characterization

AM samples usually exhibit an anisotropic non-equilibrium microstructure depending on the materials building direction. We observed the grain structures of SS 304L made by the PBF and DED methods. Figure 3 shows the optical microscopic (OM) images and the EBSD maps of SS 304L sample cross sections which are parallel to the building direction. Figs. 3 (a) and (c) show the OM images of the PBF and DED sample, respectively. The PBF sample has semicircular pattern with an average size of 100 μm in diameter, which represent the melt pools. On the other hand, the DED sample has larger melt pools with 800 μm in diameter.

EBSD observation shows the grain structure of two types of AM materials. From the EBSD measurement, the average grain size of PBF and DED samples was found to be ~40 μm and ~30 μm, respectively, which are displayed in Figs. 3 (b) and (d). Especially, the EBSD image of DED sample shows a combination of two kind grain structure: round and fine equiaxial grains in the center of the melt pool and columnar grains extending to boundary of the melt pool. This structure is the result of the high thermal gradient and cooling speed associated with laser solidification process.

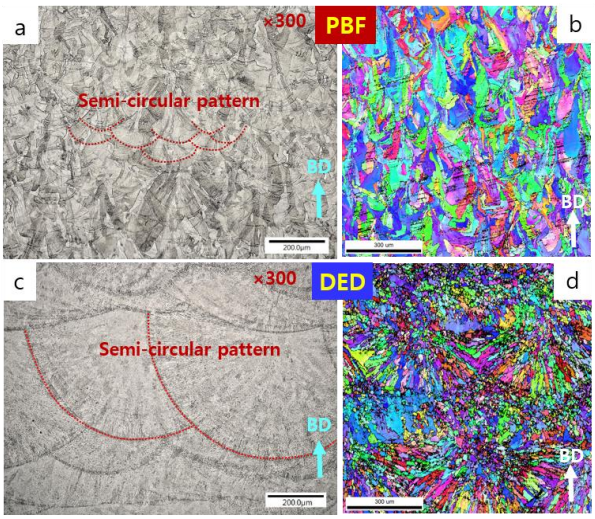

Fig. 3. OM and EBSD images of AM SS 304L samples, all cross-sections parallel to materials building direction: (a) OM – PBF, (b) EBSD – PBF, (c) OM – DED, (d) EBSD – DED

4-2. Hardness and Tensile Tests

The presence of pores in 3D-printed parts affects their mechanical properties. Therefore, we measured the pore distribution of the AM samples by observing the OM images. Fig. 4 shows the optical images of cross sections parallel to the building direction of samples. The PBF sample appears to have a higher density of pores than the DED sample. The results of the porosity analysis are shown in Table 1.

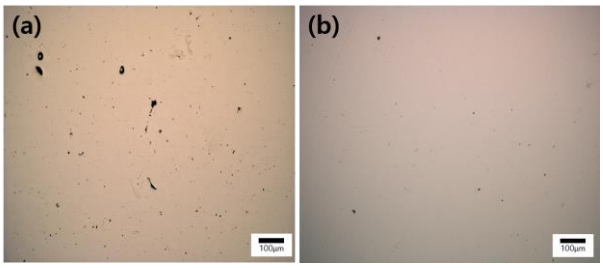

Fig. 4. Optical view of cross sections of AM SS 304L: (a) PBF, (b) DED.

TABLE I: Pore analysis of AM SS 304L samples by PBF and DED methods

	Average pore fraction (%)	Average Pore density (#/mm^2)	Max pore diameter (μm)
PBF	0.14	83	23.6
DED	0.05	41	14

The surface hardness of the samples was measured using a Micro Vickers Hardness Tester. The average hardness values are listed in Table 2, where the DED sample shows the highest value. The complex grain structures of the AM samples might affect the higher hardness rather than those of the wrought SS.

TABLE II: Vickers hardness of SS 304L samples (wrought, PBF, DED)

Vickers hardness (HV)	wrought	PBF	DED
	152.4	218.3	245.5

We performed a tensile test and compared the mechanical properties of PBF, DED and wrought samples, which are seen in Fig. 5. The yield strength and ultimate tensile strength of AM SS are higher than those of the wrought one. It should be noted that the elongation of PBF specimen decreased with increasing the yield strength. The DED specimen, however, showed higher elongation than the wrought material even though the yield strength increased. This result implies that strength-ductility tradeoff, a common phenomenon in which ductility decreases as the strength enhancement, was averted in the DED SS [13]. It indicates that the DED method can overcome the reduction of elongation caused by strengthening. As a result, the DED sample revealed the best tensile properties in both tensile strength and elongation.

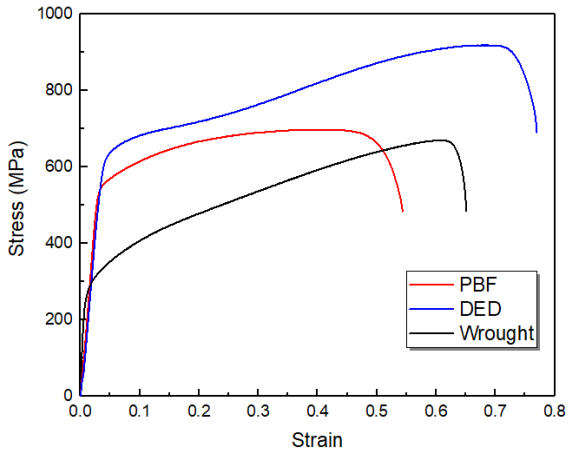

Fig. 5. Engineering stress-strain curve of wrought, PBF and DED stainless steel 304L

4-3. Pin-on-Disk Wear Test

In order to investigate the wear resistance, we measured the weight loss of three SS 304L samples from the pin-on-disk tests. The amount of weight loss of the disk is shown in Fig. 6. Wear loss of DED sample was the least among the three samples. The results of the wear test show that the hardness of the specimen and the wear loss are inversely proportional. This result satisfies the Archard wear equation, which accounts for a well-known relationship in which the wear volume and hardness are inversely proportional in a sliding wear model [14]. It implies that DED sample has a higher

wear resistance compare to Wrought and PBF. It can be seen that the weight of wear loss was diminished at 250℃. This is caused by the formation of thin oxide film at high temperature on the surfaces. This film, called the glaze layer, prevents direct metallic contact, which eventually reduces the amount of sliding wear.

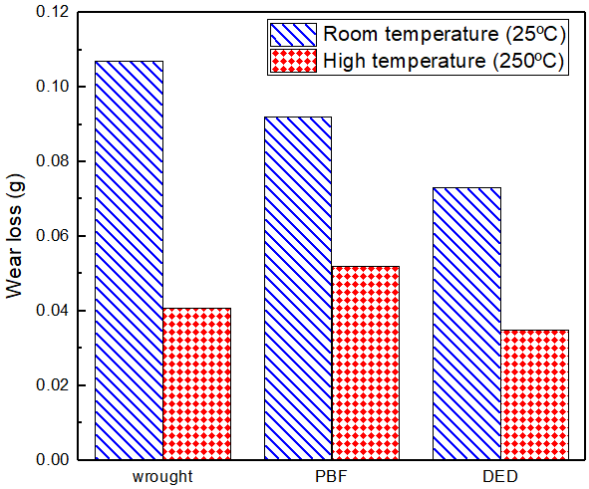

Fig. 6. Weight loss of SS 304L samples from a pin-on-disk test as a function of temperature (25°C & 250°C), including wrought, PBF and DED.

5. Conclusions

In this study, we assessed a comparative study of the effect of AM methods on microstructural, mechanical and wear behavior of the SS 304L. From this work, the following conclusions can be drawn:

1. It was found that higher density of pore is existent in the PBF sample rather than in the DED one.
2. The AM samples usually show the combination of equiaxial and columnar grains, which is dominant in the DED sample.
3. The highest properties regarding yield strength, ultimate tensile strength and hardness were obtained from the DED samples.
4. From the pin-on-disk wear test, no orientation dependency of wear behavior was observed. The DED SS specimens showed greater wear resistance among all the tested specimens at room temperature.

The DED method seems to be a good choice to manufacture the SS parts with improved mechanical and wear performance. The high performance of AM 304L is primarily caused by the finer microstructure resulting from the AM process. The generation of research data is expected to make a contribution to implementation of AM technology in the nuclear power industry.

6. Acknowledgments

This research was financially supported by the Korea Atomic Energy Research Institute (KAERI) R&D Program. The title of research project is; Technology Development for Reactor Internal Materials & Components based on 3D Printing.

REFERENCES.

[1] American Society for Testing and Materials, ASTM F2792-12a. Standard terminology for additive manufacturing technologies. ASTM International, West Conshohocken, 2012.
[2] Estelle MARC, “Analyse de la réponse tribologique d'un contact cylindre/plan soumis à des sollicitations de fretting sous chargement complexe: influence d'une solution Lithium-Bore”, universite de lyon, 2018.
[3] Gerard. R, “Ageing Management of Reactor Internals in Belgian NPPs in view of Long Term Operation”, IAEA-CN—194, 2012.
[4] W. J. Chitty and J. Ph. Vernot, “France Woodhead Publishing Limited”, Tribocorrosion issues in nuclear power generation, AREVA NP Technical Center, France, 2011.
[5] Liverani. E, et al., “Effect of selective laser melting (SLM) process parameters on microstructure and mechanical properties of 316L austenitic stainless steel, Journal of Materials Processing Technology, 2017.
6[] Sun, Zhongji, et al., “Selective laser melting of stainless steel 316L with low porosity and high build rates”, Materials & Design, 2016.
[7] De Lima, S. Sankare, “Microstructure and mechanical behaviour of laser additive manufactured AISI 316 stainless steel stringers”, Materials & Design, 2014.
[8] Bhavar, Valmik & Kattire, Prakash & Patil, Vinaykumar & Khot, Shreyans & Gujar, Kiran & Singh, Rajkumar, “A review on powder bed fusion technology of metal additive manufacturing”, 2014.
[9] simufact.com: “Additive Manufacturing Technology”, Available at: https://www.simufact.com/files/Medien/_2Produkte/2.3_Simufact_Additive/LBM%20principle%20with%20machine%20scheme.png, 2017.
[10] 3deo.co: “Metal 3D Printing The Ultimate Guide”, Available at https://news.3deo.co/metal-3d-printing-processes-directed-energy-deposition-ded, 2018.
[11] Wolff S J, Lin S, Faierson E J, et al, “A framework to link localized cooling and properties of directed energy deposition(DED)-processed Ti-6Al-4V”, Acta Materialia, 132: 106–117, 2017.
[12] American Society for Testing and Materials, ASTM G99-05. Standard Test Method for Wear Testing with a Pin-on-Disk Apparatus. ASTM International, West Conshohocken , 2005.
[13] Robert O Ritchie, “The conflicts between strength and toughness”, Nature materials, Vol.10, p.817, 2011.
[14] S.C. Lim, “The relevance of wear-mechanism maps to mild-oxidational wear”, Tribo. International, Vol.35, p.717 ,2002.